Multiple Endpoint Analysis of the 3D-Reconstituted Corneal Epithelium after Treatment with Benzalkonium Chloride: Early Detection of Toxic Damage

Aude Pauly,[1,2] *Marisa Meloni,*[3] *Françoise Brignole-Baudouin,*[1,2] *Jean-Michel Warnet,*[1,2,4] *and Christophe Baudouin*[1,4,5]

Purpose. To investigate the effects of benzalkonium chloride (BAK) on the human reconstituted corneal epithelial model (HCE) and to optimize the operating potential of this model in the field of ophthalmic toxicology.

Methods. The HCEs were treated with 0.001% to 0.5% BAK for 24 hours followed or not by a 24-hour postincubation period. To complete the histologic analysis, the authors designed a new MTT procedure to assess cellular viability. Frozen sections were analyzed by using fluorescence confocal microscopy for the presence of TUNEL, activated caspase-3, Ki67, ICAM-1, HLA-DR, E-cadherin, and occludin. Occludin gene expression was also investigated by using quantitative RT-PCR.

Results. The MTT test revealed a dose-dependent response of BAK with significant toxic effects for concentrations as low as 0.005%. Increasing BAK concentrations induced an increased number of apoptotic cells, found from the superficial to the deeper layers, with the activation of caspase-3 at 0.01% and 0.02% concentrations. The number of Ki67- and ICAM-1–positive cells increased with 0.01% BAK and with 0.001% to 0.01% BAK, respectively. BAK induced the dose-dependent disappearance of occludin in the superficial layers while increasing its gene expression up to the 0.02% BAK concentration.

Conclusions. Fluorescence techniques conjugated with confocal microscopy on 3D-reconstructed corneal epithelia were well suited for the investigation of toxicological markers such as cell junction alteration, apoptosis, cell activation, and proliferation and gave relevant results compared with the known human data. They complement the new sensitive MTT test and improve the operating potential of this new, valuable 3D model in ophthalmic toxicology. (*Invest Ophthalmol Vis Sci.* 2009;50:1644–1652) DOI:10.1167/iovs.08-2992

Chemicals, cosmetics, and pharmaceuticals have to be assessed for their irritancy potential and risk to the human eye. However, the only method accepted worldwide by regulatory authorities for the assessment of acute eye irritation potential is the Draize rabbit test,[1] which has been criticized by animal welfare advocates and its relevance, validity, and precision challenged because of the variability and low predictiveness of the human response.[2,3] This test is mainly based on scoring of observed macroscopic changes in the rabbit cornea, conjunctiva, and iris. Various scoring systems are currently accepted (Maximum Average Score [MAS], Modified Maximum Average Score [MMAS], and the Globally Harmonized System). Among the in vitro alternatives accepted in 2007, the bovine corneal opacity and permeability (BCOP),[4–7] and the isolated chicken eye (ICE)[8,9] assays were found to adequately predict severe irritancy but were not recommended to identify mild to low irritants. Therefore, the principal challenge remains the development of alternative methods suited for assessing non-severe irritants and nonirritants. The reconstructed three-dimensional (3D) model of human corneal cells (HCEs), supplied by SkinEthic Laboratories (Nice, France), was found to resemble the corneal epithelium of the human eye in morphology and thickness.[10] It was proposed as a useful alternative model to the classic Draize test[11,12] for the assessment of eye irritation potential of chemicals and cosmetic products. The toxicokinetic approach described by Doucet et al.[12,13] was based on the MTT test procedure previously published on 3D-reconstituted epidermal and corneal models. The MTT test has already been shown to constitute a rapid and cost-effective method of screening for surface toxicity of topical agents using monolayer cell cultures[14] and the procedure used on 3D-models provided a good correlation between in vitro results and MMAS values that correspond to the MAS obtained after 24 hours or more in vivo. However, because the MTT solution was placed under the construct, it could penetrate only two or three layers from the basal side, yielding results that may not correlate with histomorphologic findings in the superficial layers. This procedure may therefore underestimate any mild toxic effect occurring at the apical surface of the constructs. In the literature, systematic histologic analysis and multiple endpoint analysis (MEA) were proposed as practical responses to prevent the occurrence of false-negative MTT results.[15–17] Although MEA is a valuable approach to determine the mechanisms of eye irritation, the MTT procedure should be optimized separately so as not to neglect the cellular events occurring in the superficial layers. We believe that a small change in the MTT procedure could lead to increased sensitivity, not only making this procedure better suited for risk prediction in case of accidental exposure to the eye, but also adapting it to the prediction of low to very low irritant potential, especially when products are used repeatedly over long periods. The implementation of these very sensitive tools to predict eye irritation is critical for ophthalmologists treating patients who may be exposed to long-term induced toxicity of substances used at low concentrations in ophthalmic preparations. One of them is the widely used eyedrop preservative benzalkonium chloride (BAK), whose toxic and inflammatory effects have been demonstrated in clinical[18–24] in vivo,[20,21,25,26] and in vitro studies.[27–29] BAK

From the [1]University of Pierre et Marie Curie-Paris 6, UMR-S592, Paris, France; the [2]Department of Toxicology, Faculty of Biological and Pharmacological Sciences, University of Paris Descartes, Paris, France; [3]Vitroscreen Laboratories, Milan, Italy; [4]Quinze-Vingts National Ophthalmology Hospital, Paris, France; and the [5]Ambroise Paré Hospital, AP-HP (Assistance Publique-Hopitaux de Paris), Paris-Ile-de-France Ouest School of Medicine, University, of Versailles, Paris, France.

Supported by an unrestricted grant from INSERM (Institut National de la Santé et de la Recherche Médicale).

Submitted for publication October 10, 2008; revised November 7, 2008; accepted January 30, 2009.

Disclosure: **A. Pauly**, None; **M. Meloni**, None; **F. Brignole-Baudouin**, None; **J.-M. Warnet**, None; **C. Baudouin**, None

The publication costs of this article were defrayed in part by page charge payment. This article must therefore be marked "*advertisement*" in accordance with 18 U.S.C. §1734 solely to indicate this fact.

Corresponding author: Aude Pauly, Institut de la Vision, 17 rue Moreau, 75012 Paris; aude_pauly@yahoo.com.

is known to induce oxidative effects[30] and caspase-dependent and -independent apoptosis counteracted by an autophagic process.[31] Chronic use of preservative is responsible for apoptosis of conjunctival cells and conjunctival inflammation, which has demonstrated negative effects (e.g., on the efficacy of glaucoma surgery).[19,32]

Consequently, the use of a highly differentiated, three-dimensional epithelial system of human ocular origin is desirable for prescreening or investigating the effects of ophthalmic drugs. It frees the experimenter from interspecies differences and provides a better approach to ocular epithelial physiology than monolayer models and cells from other organs. It is also a useful alternative to animal testing, which is time consuming and often invasive and which may lack suitably sensitive tools for detecting subclinical reactions. The 3D system models not only the different effects of toxicity on specific cell types, but also the interaction between the cells and the spatial effects induced by the toxic source. Moreover, epithelial cultures at the air–liquid interface are easy to handle and facilitate in vivo-like product exposures. Some of them can inhibit the flow of ionic material such as Na-fluorescein across their surface,[33] suggesting the presence of a functional epithelial barrier, and the 3D-HCE cells were shown to express cytokeratin-3 and to include hemidesmosomes in the basal layers.[10] Different types of intercellular junctions have been identified in the corneal epithelium ex vivo. Among them, adherens junctions, comprising the E-cadherin protein, serve to anchor cells together.[34] Also, the tight junctions, originally defined as zonula occludens (ZO) and comprising occludin, ZO-1, and other proteins, are thought to provide the hydrophobic barrier preventing the free passage of molecules between adjacent epithelial cells.[35–37]

The objective of this study was to optimize the operating potential of this new epithelial model in the field of ophthalmic toxicology. Using a 0.001% to 0.1% range of BAK concentrations, we investigated in vitro the various parameters likely to be modified by the toxic substance. Since the 0.01% BAK concentration failed to induce any significant decrease in cellular viability using the classic MTT procedure and considering that this procedure could be optimized, we made modifications so as to assess, with better sensitivity, the effects of BAK on cellular viability. Then, using en face confocal microscopy on frozen sections and entire epithelia, we investigated the BAK-induced changes in the expression and spatial distribution of various cellular markers involved in intercellular junctions (E-cadherin, occludin), cell activation (CD54, HLA-DR), cell proliferation (Ki67), and apoptosis (activated caspase-3, TUNEL). In addition, we examined the effects of BAK on the mRNA expression of occludin. This study is an example of the MEA that can be used in toxicologic testing. This approach may help detect the subclinical signs of cellular toxicity that are possibly responsible for the adverse reactions associated with long-term use of ophthalmic products.

Materials and Methods

Tissue Model and BAK Treatments

The 3D-HCE model was supplied by SkinEthic Laboratories. It consists of immortalized HCE cells grown vertically on a 0.5-cm^2 inert permeable polycarbonate filter and cultivated for 5 days at the air–liquid interface in a supplemented, chemically defined medium (modified MCDB 153; SkinEthic Laboratories). At reception, the 3D-HCE cells were equilibrated for 4 hours in the defined maintenance medium provided before experiments were conducted. Thirty microliters of PBS or BAK at 0.001%, 0.005%, 0.01%, 0.02%, and 0.1% concentrations was applied on the apical surface of 3D-HCE cells for 6, 24, and 24 hours followed by a 24-hour additional recovery period (24+24 hours). The postincubation period was chosen to allow the cells to recover if toxic effects were still reversible. This treatment procedure was expected to model the defense capacity of the tissue better. The apical surface was rinsed twice with 150 μL of PBS after the treatment. Different series of 3D-HCE cells were subjected to histologic analyses after paraffin embedding and hematoxylin and eosin [H&E] staining, inclusion in OCT embedding medium (Tissue-Tek; Miles, Inc., Elkhart, IN) followed by immunofluorescence analyses on frozen sections, direct immunofluorescence labeling for en face confocal microscopic analysis, MTT testing, and RNA extraction followed by RT-PCR analysis.

MTT Test

Cellular viability was evaluated by the rapid colorimetric MTT assay, originally described by Mosmann.[38] and adapted to reconstituted tissues[13] including the 3D-HCE by Doucet et al.[11] The assay measures the activity of the mitochondrial enzyme succinyl dehydrogenase, which is expressed in living cells. The signal generated is proportional to the number of metabolically active cells.

The classic MTT procedure[13] failed to reveal significant toxicity of 0.01% BAK after 24 hours of treatment (data not shown), but we know from the histologic analysis that this concentration induces damage in the most superficial layers. Because the MTT solution was placed under the construct and could penetrate only two or three layers from the basal side (data not shown), we hypothesized that a decreased viability in the superficial layers could not be detected. We therefore modified the procedure used by Doucet et al.[11] to ensure impregnation of all cellular layers of the tissue so that cytotoxicity in the apical layers of the 3D construct would not be underestimated. The 3D-HCE cells were transferred to 24-well plates containing 300 μL of MTT solution diluted at 0.5 g/mL in the culture medium; 300 μL of the same MTT solution was applied on the apical surface of the 3D-HCE cells. The reconstituted tissues were incubated for 3 hours in an incubator at 37°C. Then, the 3D-HCE cells were transferred to 24-well plates containing 750 μL isopropanol, and 750 μL isopropanol was added to the apical surface of the 3D-HCE cells. The plates were agitated for 2 hours at room temperature. The solutions were vigorously homogenized, before the optical density (OD) was read at 570 nm versus OD690 nm. The results were expressed as a percentage of cell viability compared with the negative control. Experiments were conducted three times. The results are expressed as mean ± SD.

Histologic Analysis

The tissue constructs were fixed in 10% formalin and then embedded in paraffin. Microtome sections (Histoslide 2000; Reichert-Jung, Vienna, Austria) were subjected to H&E staining for histomorphologic analysis.

Confocal Immunofluorescence Analyses of Frozen Sections and Entire Epithelia

The construct was transferred to a Petri dish containing 500 μL of PBS and cut into two pieces under the microscope. One piece of tissue was fixed in paraformaldehyde 4% for 15 minutes before immunofluorescence labeling of the tight junction protein occludin. The other piece was embedded in OCT embedding medium and frozen at −80°C. Vertical sections (10 μm thick) were cut with a cryotome (CM 3050s; Leica Microsystems AG, Wetzlar, Germany) and stored at −20°C until staining.

The sections were subjected to immunofluorescence with antibodies against E-cadherin, occludin, ICAM-1, HLA-DR, Ki67, and activated caspase-3 as follows. The samples were fixed with 4% paraformaldehyde (PFA) for 5 minutes and then permeabilized with 0.01%-diluted Triton X-100 (Sigma-Aldrich, St. Louis, MO) for 5 minutes, except for occludin, E-cadherin, and CD54 labeling of frozen sections. After they were rinsed with 1% BSA-PBS, different sets of primary antibodies were added to 1% BSA-PBS: the rabbit anti-occludin IgG1 (1:50; Santa Cruz Biotechnology, Santa Cruz, CA), the rabbit anti-activated caspase-3 (1:50; BD-PharMingen, San Diego, CA), and the mouse anti-human IgG1 against E-cadherin (1:50; DakoCytomation, Glostrup, Denmark).

After 1 hour of incubation, the sections were rinsed twice in 1% BSA-PBS and incubated again for 1 hour in the dark with Alexa488-conjugated goat anti-mouse IgG at a 1:500 dilution or Alexa488-conjugated goat anti-rabbit IgG at a 1:500 dilution (Invitrogen-Molecular Probes, Eugene, OR). A terminal deoxynucleotidyl transferase-mediated dUTP nick-end labeling (TUNEL) assay (Roche Diagnostics, Meylan, France) was used to detect apoptosis in the tissue layers. After three washes in PBS, the nuclei were labeled with propidium iodide or DAPI and mounted in an anti-fade medium (Vectashield; Vector Laboratories, Burlingame, CA). During all the en face immunofluorescence analysis steps, the epithelial side was kept upward to avoid damage. The samples were analyzed under a laser confocal microscope (E800, PCM 2000; Nikon, Champigny-sur-Marne, France).

Quantification

CD-54–, Ki67-, activated caspase-3–, and TUNEL-positive cells were quantified manually, using a microscopic grid on images under ×400 magnification. The results were expressed as the mean cell number per millimeter of epithelial length (mm EL). Standard deviations are indicated.

Occludin mRNA Expression Study

BAK is known as a penetration enhancer. Because occludin is known as one of the most specific tight junction proteins, we focused on its gene expression in response to BAK treatment. The 0.05% BAK concentration was added in this set of experiments so as to better characterize the change in the occludin expression pattern found between the 0.02% and the 0.1% BAK concentrations. Also, the time of 6 hours was added for more comprehensive results.

After each time point of treatment, RNA was extracted from the 3D-HCE cells (RNAqueous; Applied Biosystems, [ABI] Monza, Italy), according to the manufacturer's protocol. Briefly, the tissue was lysed with a high-concentration guanidinium salt-containing buffer to inactivate endogenous RNase and then homogenized. Total RNA was isolated on a spin column and then eluted in a low-ionic-strength solution.

The cDNAs were then synthesized from 2 μg RNA template in a 20-μL reaction (High-Capacity cDNA Reverse Transcription Kit; ABI). The master mix used for the reverse transcription contained 2 μL 10× RT buffer, 0.8 μL 25× dNTP mix, 2 μL 10× random primers, 1 μL RT (Multiscribe; ABI), 1 μL RNase inhibitor, and 3.2 μL nuclease-free water. Ten microliters of RNA was added to the master mix and then subjected to reverse transcription in a thermal cycler (Prism 7500 Real Time PCR System; ABI). The cDNA was amplified with *Taq* polymerase (*Taq*Man Universal PCR Master Mix; Invitrogen) and the following gene expression assays (*Taq*Man; Invitrogen): the human GAPDH probe GAPDH Hs99999905_m1 (calibrator gene) and the human occludin probe OCLN Hs00170162_m1 (occludin gene; *Taq*man probe; Invitrogen). PCR amplifications were performed with 25 ng of cDNA in 25 μL of total volume. Briefly, we used 12.5 μL of 2× PCR master mix (*Taq*Man Universal PCR Master Mix; Invitrogen), 1.25 μL of 20× gene expression assay, 6.25 μL of water, and 5 μL of cDNA. The PCR conditions were 95°C for 10 minutes (AmpliTaq Gold DNA Polymerase Activation; ABI) followed by 40 amplification cycles on a real-time PCR system (95°C for 15 seconds and 60°C for 1 minute; Prism 7500; ABI). For each sample, analyses were performed in triplicate. Expression rates were expressed as relative quantification data (RQ), with changes considered significant when RQ was decreased or increased twofold compared with the control.

Statistical Analysis

Statistical comparisons of control and treatment groups for MTT data and quantification of Ki67-, activated caspase-3–, and TUNEL-positive cells were performed by two-way analysis of variance (ANOVA), followed, if necessary, by multiple pair-wise comparisons with the Bonferroni adjustment (Statview V for Windows; SAS Institute, Cary, NC).

Results

Histologic Analysis

The morphology of the control consisted of a layer of nonkeratinized, more or less flattened superficial cells, an intermediate cell layer, where cells displayed lateral cytoplasmic extension similar to the wing cells, and a basal layer presenting regular column cuboidal cells. After 72 hours of treatment with any concentration of BAK, the histologic analysis as well as the MTT test revealed drastic cell death in all cellular layers associated with low viability levels (data not shown). The histologic analysis of the 3D-HCE revealed a dose- and time-dependent effect of BAK, with a reduced epithelial thickness and the presence of an increasing number of necrotic cells from the apical to the basal layers with increasing BAK concentrations, compared to the control (Fig. 1). BAK at 0.01% induced modification of the superficial layer continuity, nucleus condensation, and vacuole formation in the superficial epithelial layer after 24 hours of treatment. These signs were more pronounced after the 24-hour postincubation period. With 0.1%

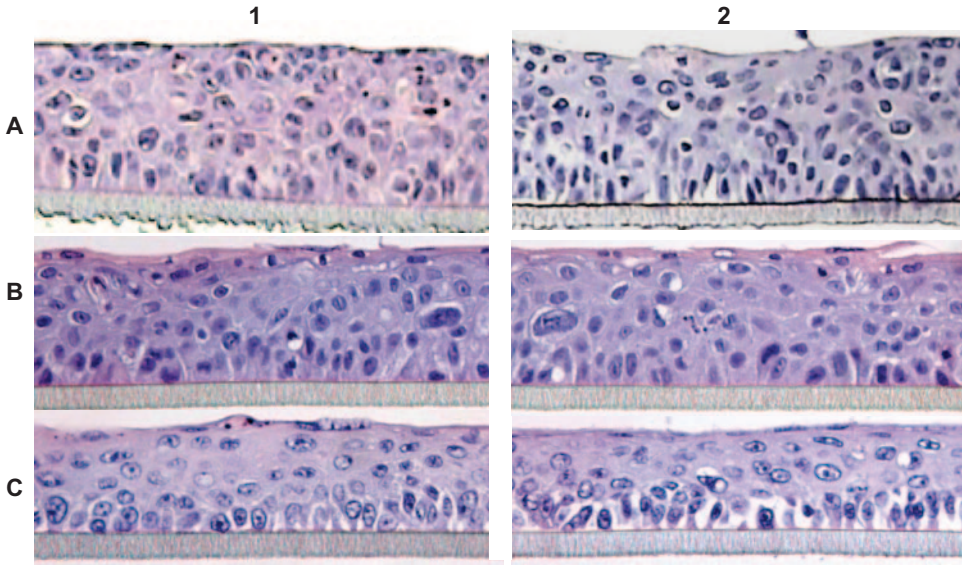

Figure 1. Histologic analyses of (**A**) PBS-, (**B**) 0.01% BAK–, and (**C**) 0.1% BAK–treated 3D-HCE cells after 24 hours of treatment with (2) or without (1) a 24-hour postincubation period. The morphology of the control consisted of a layer of nonkeratinized, more or less flattened, superficial cells, an intermediate cell layer, where cells displayed lateral cytoplasmic extension similar to the wing cells and a basal layer presenting regular column cuboidal cells (**A1**, **A2**). The 24-hour treatment with 0.01% BAK induced reduced epithelial thickness, nucleus condensation and vacuole formation in the apical cells (**B1**); the cells did not recover after the 24-hour postincubation period (**B2**). BAK at 0.1% induced cell damage and nucleus condensation in all epithelial cell layers after 24 hours of treatment (**C1**); the cells did not recover after the 24-hour postincubation period (**C2**).

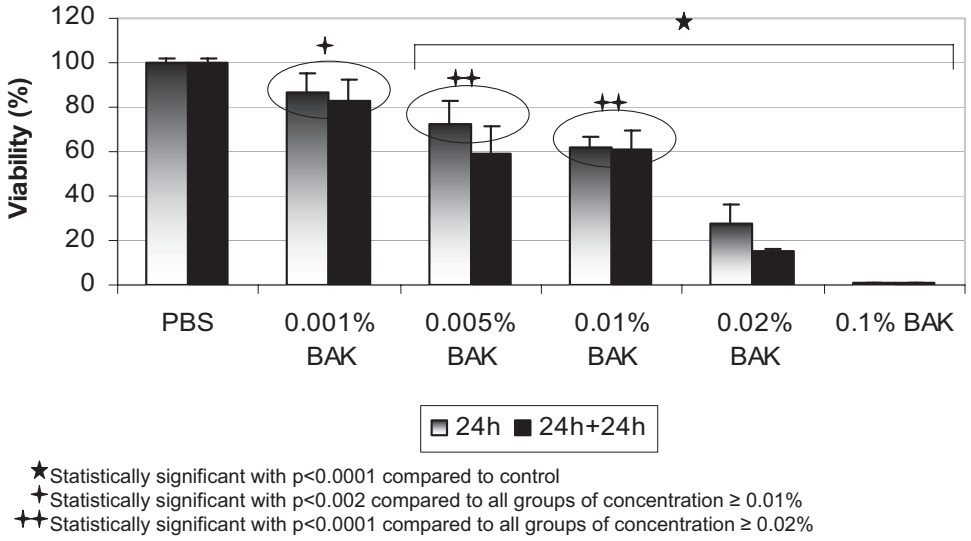

FIGURE 2. Cellular viability of PBS, 0.001%, 0.005%, 0.01%, 0.02%, and 0.1% BAK-treated 3D-HCE after 24 hours of treatment with and without the 24-hour postincubation period. BAK induced a dose-dependent decrease in cellular viability as assessed by the MTT test. This decrease was considered significant for concentrations as low as 0.005% compared to the control and according to multiple pair-wise comparisons using the Bonferroni adjustment ($n = 3$).

BAK, all cellular layers were affected as early as 24 hours, with most of the cells detaching from each other and undergoing cell death after the 24-hour postincubation period.

Modified MTT Test

BAK induced a dose-dependent significant decrease in cellular viability as assessed by the MTT test after 24 hours and 24+24 hours (Fig. 2). The 0.001% BAK concentration tended to reduce cell viability at 86.6% and 82.6% at 24 hours and 24+24 hours, respectively. The 0.005% to 0.1% range of concentrations showed significant cytotoxic effects on 3D-HCE cells ($P < 0.0001$ compared to control), with 0.005% BAK, 0.01% BAK, and 0.02% BAK inducing, respectively, 72.8%, 61.7%, and 27.3% viability at 24 hours and 59.8%, 60.9%, and 15.3% viability at 24+24 hours. The damage tended to be greater after the 24-hour postincubation period, and all 3D-HCE cells were found to be dead with 0.1% BAK. When only two values were used for each treatment group, the MTT test discriminated between the toxicity levels of 0.001% BAK versus 0.01% BAK, 0.005% BAK versus 0.01% BAK, and 0.01% BAK versus 0.02% BAK.

Immunofluorescence Analysis and Quantification on Frozen Sections

Rare, homogenously disseminated, TUNEL-, and caspase-3–positive cells were found in the control 3D-HCE cultures (Figs. 3A1, 3A2). BAK concentrations ranging from 0.01% to 0.1% significantly increased the number of TUNEL-positive cells in a dose-dependent manner with 83, 85, and 310 cells/mm EL after 0.01%, 0.02%, and 0.1% BAK treatments, respectively (Fig. 4A). At these three concentrations, the cells did not recover after the postincubation period, and more cells tended to undergo apoptosis with 140, 261, and 390 cells/mm EL, respectively. Of

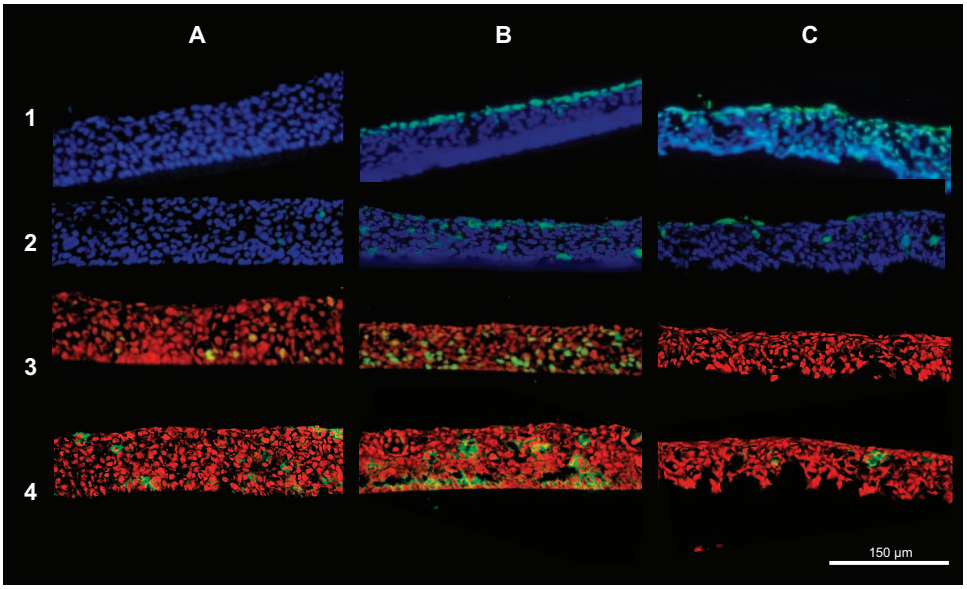

FIGURE 3. Immunolocalization of TUNEL (*row 1*), activated caspase-3 (*row 2*), Ki67 (*row 3*), and ICAM-1 (*row 4*) *green* positive cells. (**A1**) TUNEL immunostaining of 3D-HCE cells showing an epithelium disclosing no or very rare apoptotic cells after PBS treatment; (**B1**) apoptotic cells in the most apical cell layer; and (**C1**) a great number of apoptotic cells in all cellular layers. (**A2**) Activated caspase-3 immunostaining showing an epithelium with no or rare positive cells after PBS treatment; (**B2**) with positive cells distributed in all cellular layers after 0.02% BAK treatment for 24 hours; and (**C2**) with few positive cells throughout the epithelium after 0.1% BAK treatment for 24 hours. (**A3**) Ki67 immunostaining showing an epithelium with proliferating cells not restricted to the basal layer after PBS treatment for 24 hours; (**B3**) numerous proliferating cells, with a great number located in the basal layer after 0.01% BAK treatment for 24 hours; and (**C3**) disclosing no proliferating cells after 24 hours of treatment with 0.1% BAK. ICAM-1 immunostaining showing an epithelium (**A4**) with ICAM-1–positive cells after PBS treatment; (**B4**) with an increased number of ICAM-1–positive cells after 0.01% BAK treatment; and (**C4**) with few remaining ICAM-1–positive cells after 0.1% BAK treatment. The nuclei were stained with DAPI (*blue*, *rows 1* and *2*) or propidium iodide (PI, *red*, *rows 3* and *4*).

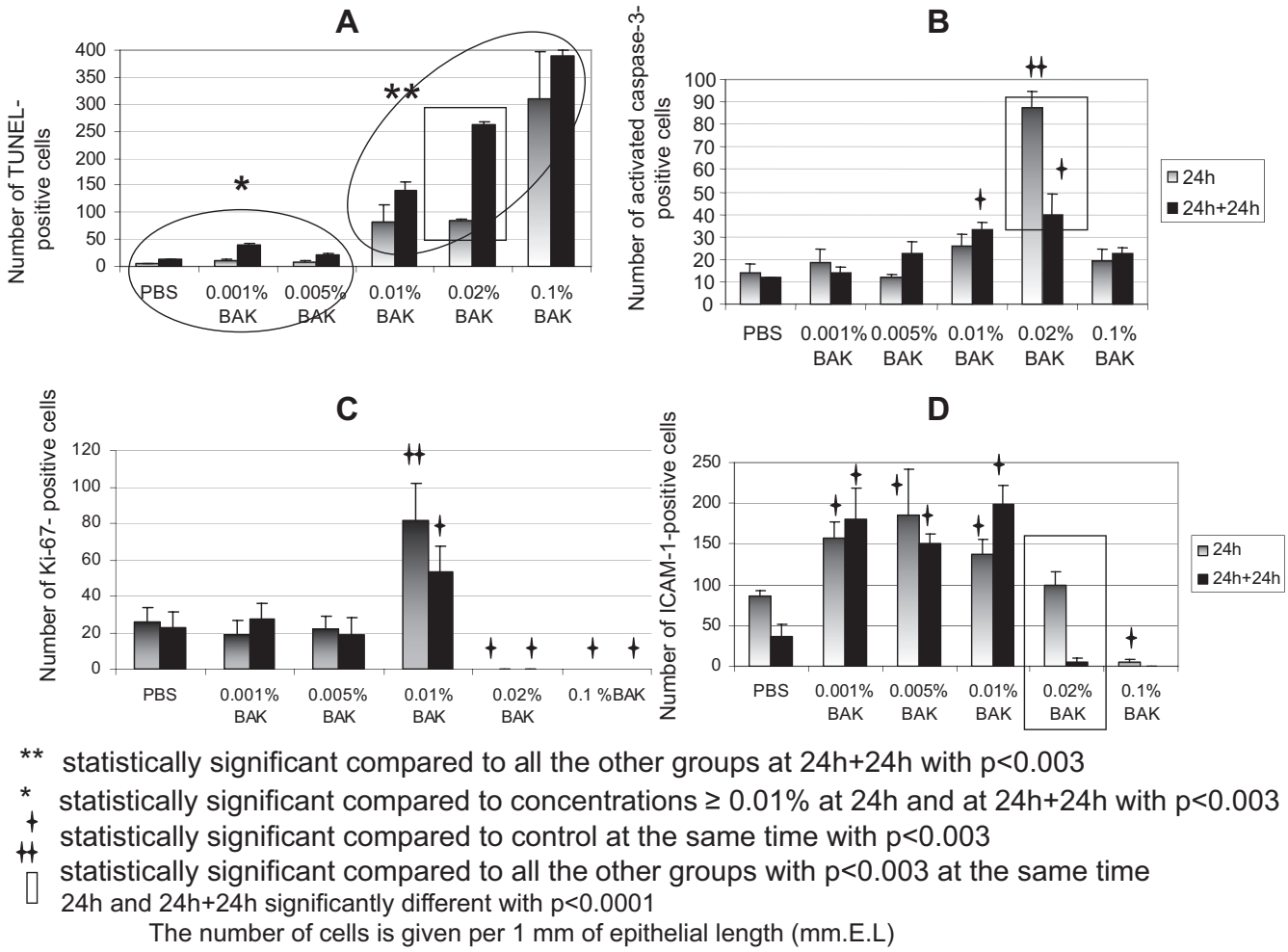

FIGURE 4. Quantification of TUNEL, activated caspase-3–, Ki67-, and ICAM-1–positive cells after 24 hours of treatment with PBS or BAK followed or not by a 24-hour postincubation period. (**A**) The quantification of TUNEL-positive cells shows BAK-induced apoptosis with a dose-dependent effect reaching significance for 0.01% BAK and higher concentrations. (**B**) BAK at 0.01% and 0.02% significantly increased the number of activated caspase-3–positive cells at 24 hours, and at 24+24 hours compared with control cells, respectively. (**C**) A pool of Ki67-expressing cells was found in the control group. The number of proliferating cells was significantly increased by 24-hour 0.01% BAK treatment. This number, although decreasing slightly after the 24-hour postincubation period, remained significantly higher than in the control. After 0.02% and 0.1% BAK treatments, no proliferating cells could be counted because most of the cells underwent cell death. (**D**) ICAM-1–expressing cells were found in the control group. After 24 hours of treatment with BAK concentrations ranging from 0.001% to 0.01%, the number of these positive cells significantly increased with and without the 24-hour postincubation period. The number of ICAM-1–expressing cells significantly decreased during the 24-hour postincubation period after 24 hours of treatment with 0.02% BAK. After 0.1% BAK treatment, only a few cells still expressed ICAM-1. Mean ± SD are represented.

interest, increasing BAK concentrations induced apoptosis in an increasing number of cellular layers, from the most superficial to the deepest basal layers (Figs. 3A1–C1). The number of activated caspase-3–positive cells increased significantly at 24 hours after 0.02% BAK treatment (87 cells/mm EL) and at 24+24 hours after 0.01% (33 cells/mm EL) and 0.02% BAK (39 cells/mm EL) treatments (Figs. 3B2, 4B). These cells were mainly located in the most superficial layer (Figs. 3A2–C2). Approximately, 21 cells/mm EL were found to be positive for Ki67 in 3D-HCE cells treated with PBS (Fig. 4C). These cells were not restricted to the basal layer, but few of them were found in the suprabasal layers (Fig. 3A3). The 24-hour treatments with 0.001% and 0.005% BAK did not significantly change the number of proliferating cells. However, the 0.01% BAK concentration significantly increased this number at levels as high as 81 and 53 cells/mm EL at 24 hours and 24+24 hours, respectively. Most of them were found in the basal layer (Fig. 3B3, 4C), and no proliferating cells were observed after 0.02% and 0.1% BAK treatments (Fig. 3C3). Control 3D-HCE cultures were found to express CD54 (ICAM-1) at levels of approximately 12 cells/mm EL (Figs. 3A4, 4D). After 24 hours of treatment with concentrations ranging from 0.001% to 0.01%, BAK significantly increased the number of CD54-positive cells ($P < 0.003$ compared with control) at levels greater than 137 cells/mm EL, with positive cells mainly located in the basal layers (Figs. 3B4). The number decreased to 98 cells/mm EL after 0.02% BAK treatment. The decrease reached significance with 0.1% BAK ($P < 0.003$ compared to control) at 24 hours and 24+24 hours. Of note, the postincubation period appeared to be critical for the 0.02% BAK concentration, as it showed a significant decrease in CD54- and activated caspase-3–positive cells compared with the treatment without a postincubation period. Neither HLA-DR nor E-cadherin was detected in the 3D-HCE cultures treated with PBS or BAK (data not shown).

En Face Confocal Microscopic Analysis of Occludin Protein Expression

En face confocal microscopic analysis of 3D-HCE cultures treated with PBS revealed a fine membrane immunostaining of

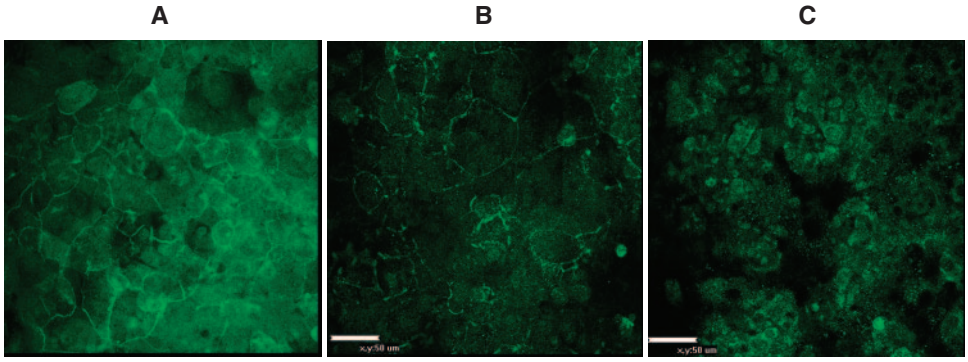

FIGURE 5. Immunofluorescence analysis of occludin protein expression by using en face confocal microscopy after treatment with PBS (**A**), 0.005% BAK (**B**), and 0.01% BAK (**C**) for 24 hours. The epithelium showed a fine occludin staining in the most superficial large cells, forming a continuous ring around them (**A**). After treatment with 0.005% BAK for 24 hours, the epithelia showed a persistent occludin expression in the apical cells (**B**), which disappeared after treatment with 0.01% BAK for 24 hours (**C**), leaving a diffuse cytoplasmic staining of occludin visible in the wing cells. Note that the undulation of the epithelium gives artifactual images of some epithelial defects, but the cell borders are visible when focusing.

occludin in the large superficial cells, forming a ring around the cells (Fig. 5). A slight occludin staining was also founded in the deeper cell layers (data not shown). After treatment with 0.001% and 0.005% BAK for 24 hours, a persistent membrane staining in the superficial layers was observed, but it disappeared at 0.01% and more concentrated BAK solutions. After the 24-hour postincubation period, no significant change in occludin protein distribution was found compared with treatment without the postincubation period (data not shown).

Occludin mRNA Expression Assessed by RT-PCR

BAK showed dose- and time-dependent effects on occludin gene expression, with inverse kinetic expression patterns for the 0.001% to 0.02% and the 0.05% to 0.1% ranges of concentrations (Fig. 6). When increasing the duration of treatment (6–24 hours) or adding a postincubation period (24+24 hours), occludin gene expression tended to increase at the low range of concentrations, whereas it decreased at the high range of concentrations. The very low 0.001% and 0.005% BAK concentrations were unable to increase occludin gene expression at 24 hours but tended to increase this expression at 24 hours of treatment followed by the 24-hour postincubation period. At 24 hours, the 0.01% and 0.02% BAK concentrations upregulated the occludin gene expression at levels reaching 1.9- and 2.6-fold the control level, respectively. This expression increased to a greater extent at 24+24 hours with an RQ of 3.3 and 6, respectively. The highest 0.05% and 0.1% BAK concentrations induced increased expression levels at the early time of 6 hours with a RQ of 3.2 and 2.9, respectively. Then, for both concentrations, occludin expression was decreased at levels still greater than the control at 24 hours and less than the control at 24+24 hours. During the 6-hour treatment, occludin mRNA expression increased with increasing BAK concentrations up to 0.05%. Then, the expression decreased at the highest 0.1% concentration.

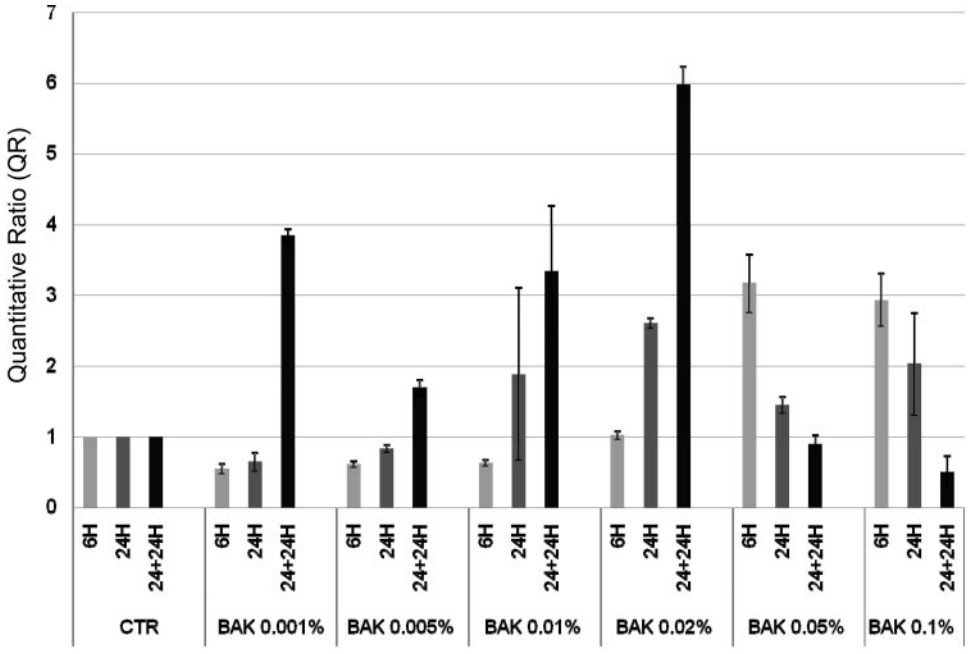

FIGURE 6. Quantitative analysis of occludin mRNA expression in 3D-HCE treated with BAK. BAK concentrations ranging from 0.001% to 0.02% induced a dose- and time-dependent increased expression of occludin mRNA in 3D-HCE cells, whereas for the two next higher BAK concentrations—0.05% and 0.1%—the expression seemed to decrease with higher doses and longer treatment periods. Twofold quantitative ratios (QR) were considered significant.

Discussion

In the rabbit Draize test, the eye irritancy score is strongly influenced by the response of the cornea, which accounts for approximately 75% of the overall score. Because of the problems of interspecies differences and given that its structure is similar to the living human corneal epithelium,[10] the 3D-HCE cell was thought to be a good surrogate for in vivo testing in the field of ocular irritation and ocular safety assessment. A relatively small number of large-scale studies have focused on the evaluation of this model. Doucet et al.[12] tested 65 cosmetic products and 35 chemicals and demonstrated a good correlation between MMAS values generated by the Draize test and in vitro results using the 3D-HCE system. In 2006, a multicenter prevalidation study was conducted to assess the ability of 3D-HCE to assess the eye irritating potential of chemicals using individual rabbit data described in the ECETOC (European Centre for Ecotoxicology & Toxicology of Chemicals) data bank[17,39] and in 2008.[40] The authors found the model to be a quality-controlled and easy-to-perform test system, with a high level of reproducibility. They emphasized that the selection of quality in vivo data on eye irritation is one of the major issues for the (pre)validation process of new in vitro methods and provided a proof of principle that the 3D-HCE system can help discriminating between eye irritants and nonirritants. However, Van Goethem et al.[17] recommended considering additional protocol modifications that may increase the discriminative power of the assay and indicated that false-negative results could be prevented by performing histologic analysis when irritants fail to induce a significant reduction in the MTT-determined viability. MEA were therefore proposed for testing mild irritants, since the tissue viability might remain unaffected, resulting in false-negative results.[15–17] Although we agree that an additional endpoint may help differentiate the mechanisms of irritation and also increase confidence in negative results, we kept in mind that numerous studies confirmed the hypothesis that area and depth of chemical-induced corneal injury correlates with cell death and can predict the extent of subsequent ocular responses.[41–47] It is therefore important to ensure that the methods for assessing cell viability in in vitro models are sufficiently sensitive. In the present study, we optimized the classic MTT protocol used for irritation assessment to increase its sensitivity and more accurately correlate with histologic findings. With this new procedure, we demonstrated that BAK induced a significant dose-dependent decrease of cell viability, with worsened effects after a 24-hour postincubation period for concentrations greater than 0.005%. These results correlated with the number of TUNEL-positive cells and correlated inversely with the number of Ki67-positive cells. This was consistent with our previously published study showing a dose-dependent increase in epithelial apoptosis in rat conjunctival brushings.[20] Moreover, the MTT test succeeded in detecting decreased cellular viability for concentrations as low as 0.005% BAK, whereas the former procedure failed to detect the effects of a 0.01% BAK concentration at 24 hours. This new, more sensitive MTT procedure is therefore expected to better predict potential adverse effects that may occur with the long-term use of ophthalmic products. It may also help optimize the protocol currently used for acute eye irritation assessment and help future validation studies. Indeed, one prediction model currently proposed to distinguish irritants from nonirritants was defined based on a viability cutoff value of 60%.[17] The use of a more sensitive MTT protocol may thus decrease this cutoff value and enlarge the scale for discriminating mild and moderate irritants. Of note, low doses of BAK induced apoptosis restricted to the superficial cell layers and proliferation mainly located in the basal layers, whereas high doses of BAK induced apoptosis in all cellular layers, including the deepest one, and hindered cell proliferation. BAK induced cell apoptosis, at least partly mediated by caspases, as demonstrated by increased activated caspase-3–positive cells with 0.01% and 0.2% concentrations. With 0.1% BAK, activated caspase-3 was not detected, probably because most of the cells were already undergoing apoptosis and because the activation of caspase-3 precedes the induction of apoptosis. It is noteworthy that BAK used at the low 0.001% to 0.01% concentrations seemed to elicit a defense response by increasing Ki67 and ICAM-1 expression as well as by increasing occludin mRNA expression; Ki67 distribution patterns were modified by 0.01% BAK only. BAK showed dose- and time-dependent effects on occludin gene expression, with inverse toxicokinetic profiles observed at the 0.001% to 0.02% and the 0.05% to 0.1% ranges of BAK concentrations. This suggests that for concentrations greater than or equal to 0.05%, the cellular defense system was no longer able to respond for treatments exceeding 6 hours.

Previous studies have already described the distribution of TJ-related protein occludin in rat,[48] rabbit,[35,49] and human corneal epithelia[50–51] as well as in human corneal cell cultures.[37,52] Our results agreed closely with those in these studies, since we found a strong membrane occludin staining in the most apical superficial cells of the control 3D-HCE cultures. BAK induced the dose-dependent disappearance of occludin, suggesting the disruption of the epithelial tight junctions in the superficial cells. These results are consistent with the known enhancer properties of BAK used to increase corneal penetration of active compounds[53] and they confirmed the results of other studies showing that the occludin distribution in monolayer cultures could be altered by a chemical treatment.[54,55] However, in two very recent studies, the expression of functional tight junctions, which is usually characterized by electrophysiological parameters such as transepithelial electric resistance (TEER), has been investigated in various corneal models including the 3D-HCE model (SkinEthic Laboratories). The studies reported that only one of these models, the HCE-T system, which is also based on transformed human corneal epithelial cells,[56] exhibited epithelial tightness and functional integrity, whereas the TEER values of the other models were far below the TEER values reported for isolated cornea.[57,58] These results were confirmed in permeation studies, with permeation coefficients that were increased by about 10-fold relative to the isolated cornea. In eye irritation testing, because intrinsic cytotoxicity potential of chemicals is a decisive factor affecting cornea after contact, the evaluation of cell viability remains the principal evaluation endpoint and epithelial barrier properties and compound permeability are typically not an issue. The permeation studies suggested, however, that the differentiation in most of the today available 3D ocular models does not occur as completely as in the human corneal epithelium.

ICAM-1 is not expressed on normal corneal epithelium. However, we found the expression of ICAM-1 in our control 3D-HCE cultures. This result was consistent with that in previous work on cultured HCE cells[59] that demonstrated ICAM-1 to be involved in corneal epithelial cell movement.[60] The BAK-induced overexpression of ICAM-1 on 3D-HCE suggests that it can contribute to corneal epithelial cell injury by aiding the attachment of inflammatory cells such as eosinophils, which express the receptor for ICAM-1 and the β2 integrins (CD11a, -b ,-c/CD18). Ki67 protein expression was observed in the nuclei of a few basal cells within the central and peripheral corneal epithelium of human donors, suggesting that individual cells within this layer undergo asynchronous cell division to replace cells lost from the epithelial surface.[61] Organotypic epidermal and oral cultures demonstrated an increased proliferation pattern (Ki67 staining) in basal and suprabasal layers after exposure to acetone and low concentrations of sodium lauryl sulfate, respectively.[62,63] Our results are in agreement

with these studies and suggest that mild to moderate stress can trigger proliferation as a mechanism of tissue defense. Finally, neither HLA-DR nor E-cadherin was detected in control and treated 3D-HCE cells.

Taken together, these results suggest that the MEA and the use of our modified, more sensitive MTT protocol will be useful for the preclinical irritation screening of new ophthalmic products in this type of tissue model. In particular, this approach may be a better predictor of the subclinical signs of ocular inflammation that occur in patients treated for long periods of time, such as patients with glaucoma whose ocular surface has shown widespread inflammatory changes and clinical impairment.[18,19,21–24,64–66] In further studies, it would be interesting to examine the recovery time for such treated cultures, and these techniques could be extended to other markers, to further investigate the mechanisms associated with various classes of drug compounds. More generally, this model must be further characterized so as to precisely define its limits and the purposes for which it can be used. It is noteworthy that the 3D-HCE model has not yet been accepted or even validated by the European Centre for the Validation of Alternative Methods (ECVAM) for eye irritation testing. Nevertheless, ECVAM prevalidation studies continue[40] to prepare this test model for further progression to a formal validation.

References

1. Draize JH, Woodward G, Calvery HO. Methods for the study of irritation and toxicity of substances applied topically to the skin and mucous membranes. *J Pharmacol Exp Ther.* 1944;82:377–390.
2. Wilhelmus KR. The Draize eye test. *Surv Ophthalmol.* 2001;45:493–515.
3. Curren RD, Harbell JW. Ocular safety: a silent (in vitro) success story. *Altern Lab Anim.* 2002;30(suppl 2):69–74.
4. Gautheron P, Dukic M, Alix D, Sina JF. Bovine corneal opacity and permeability test: an in vitro assay of ocular irritancy. *Fundam Appl Toxicol.* 1992;18:442–449.
5. Gautheron P, Giroux J, Cottin L, et al. Interlaboratory assessment of the bovine corneal opacity and permeability (BCOP) assay. *Toxicol In Vitro.* 1994;8:381–392.
6. Sina JF, Galer DM, Sussman RG, et al. A collaborative evaluation of seven alternatives to the Draize eye irritation test using pharmaceutical intermediates. *Fundam Appl Toxicol.* 1995;26:20–31.
7. Ubels JL, Paauw JD, Casterton PL, Kool DJ. A redesigned corneal holder for the bovine cornea opacity and permeability assay that maintains normal corneal morphology. *Toxicol In Vitro.* 2002;16:621–628.
8. Prinsen MK, Koeter HB. Justification of the enucleated eye test with eyes of slaughterhouse animals as an alternative to the Draize eye irritation test with rabbits. *Food Chem Toxicol.* 1993;31:69–76.
9. Prinsen MK. The chicken enucleated eye test (CEET): a practical (pre)screen for the assessment of eye irritation/corrosion potential of test materials. *Food Chem Toxicol.* 1996;34:291–296.
10. Nguyen DH, Beuerman RW, De Wever B, Rosdy M. Three-dimensional construct of the human corneal epithelium for in vivo toxicology. In: Salem H, Katz S, eds. *Alternative Toxicological Methods*. Boca Raton, FL: CRC Press; 2003;147–159.
11. Doucet O, Lanvin M, Zastrow L. A new in vitro human epithelial model for assessing eye irritating potential of formulated cosmetic products. *In Vitro Mol Toxicol.* 1998;11:273–283.
12. Doucet O, Lanvin M, Thillou C, et al. Reconstituted human corneal epithelium: a new alternative to the Draize eye test for the assessment of the eye irritation potential of chemicals and cosmetic products. *Toxicol in Vitro.* 2006;20(4):499–512.
13. Doucet O, Robert C, Zastrow L. Use of a serum-free reconstituted epidermis as a skin pharmacological model. *Toxicol In Vitro.* 1996;10:305–313.
14. Sosa AB, Epstein SP, Asbell PA. Evaluation of toxicity of commercial ophthalmic fluoroquinolone antibiotics as assessed on immortalized corneal and conjunctival epithelial cells. *Cornea.* 2008;27(8):930–934.
15. Guest R, Seaman CW, De Wever B, Cappadoro M, Whittingham A, Prusiewicz CM. The use of a human reconstituted corneal epithelium model for the occupational hazard assessment of pharmaceutical process materials. *The Toxicologist: an Official Publication of the Society of Toxicology.* 2004;(abstracts of the annual meeting)78:269.
16. Meloni M, Dalla Valle P, Cappadoro M, de Wever B. The importance of multiple endpoint analysis (MEA) using reconstituted human tissue models for irritation and biocompatibility assays. *INVITOX Abstract Book.* 2002:4–7.
17. Van Goethem F, Adriaens E, Alepee N, et al. Prevalidation of a new in vitro reconstituted human cornea model to assess the eye irritating potential of chemicals. *Toxicol In Vitro.* 2006;20:1–17.
18. Baudouin C, Hamard P, Liang H, et al. Conjunctival epithelial cell expression of interleukins and inflammatory markers in glaucoma patients treated over the long term. *Ophthalmology.* 2004;111:2186–2192.
19. Baudouin C, Liang H, Bremond-Gignac D, et al. CCR 4 and CCR 5 expression in conjunctival specimens as differential markers of T(H)1/ T(H)2 in ocular surface disorders. *J Allergy Clin Immunol.* 2005;116:614–619.
20. Pauly A, Brignole-Baudouin F, Labbe A, et al. New tools for the evaluation of toxic ocular surface changes in the rat. *Invest Ophthalmol Vis Sci.* 2007;48:5473–5483.
21. Pisella PJ, Fillacier K, Elena PP, Debbasch C, Baudouin C. Comparison of the effects of preserved and unpreserved formulations of timolol on the ocular surface of albino rabbits. *Ophthalmic Res.* 2000;32:3–8.
22. Asbell PA, Potapova N. Effects of topical antiglaucoma medications on the ocular surface. *Ocul Surf.* 2005;3(1):27–40.
23. Leung EW, Medeiros FA, Weinreb RN. Prevalence of ocular surface disease in glaucoma patients. *J Glaucoma.* 2008;17(5):350–355.
24. Fraunfelder FW. Corneal toxicity from topical ocular and systemic medications. *Cornea.* 2006;25(10):1133–1138.
25. Kahook MY, Noecker R. Quantitative analysis of conjunctival goblet cells after chronic application of topical drops. *Adv Ther.* 2008;25(8):743–751.
26. Kahook MY, Noecker RJ. Comparison of corneal and conjunctival changes after dosing of travoprost preserved with sofZia, latanoprost with 0.02% benzalkonium chloride, and preservative-free artificial tears. *Cornea.* 2008;27(3):339–343.
27. Baudouin C, Riancho L, Warnet JM, Brignole F. In vitro studies of antiglaucomatous prostaglandin analogues: travoprost with and without benzalkonium chloride and preserved latanoprost. *Invest Ophthalmol Vis Sci.* 2007;48:4123–4128.
28. Guenoun JM, Baudouin C, Rat P, et al. In vitro comparison of cytoprotective and antioxidative effects of latanoprost, travoprost, and bimatoprost on conjunctiva-derived epithelial cells. *Invest Ophthalmol Vis Sci.* 2005;46:4594–4599.
29. Guenoun JM, Baudouin C, Rat P, et al. In vitro study of inflammatory potential and toxicity profile of latanoprost, travoprost, and bimatoprost in conjunctiva-derived epithelial cells. *Invest Ophthalmol Vis Sci.* 2005;46:2444–2450.
30. De Saint Jean M, Brignole F, Bringuier AF, et al. Effects of benzalkonium chloride on growth and survival of Chang conjunctival cells. *Invest Ophthalmol Vis Sci.* 1999;40:619–630.
31. Buron N, Micheau O, Cathelin S, et al. Differential mechanisms of conjunctival cell death induction by ultraviolet irradiation and benzalkonium chloride. *Invest Ophthalmol Vis Sci.* 2006;47:4221–4230.
32. Calonge M, Diebold Y, Saez V, et al. Impression cytology of the ocular surface: a review. *Exp Eye Res.* 2004;78:457–472.
33. Kahn CR, Young E, Lee IH, Rhim JS. Human corneal epithelial primary cultures and cell lines with extended life span: in vitro model for ocular studies. *Invest Ophthalmol Vis Sci.* 1993;34:3429–3441.
34. Gumbiner BM. Cell adhesion: the molecular basis of tissue architecture and morphogenesis. *Cell.* 1996;84:345–357.
35. Wang Y, Chen M, Wolosin JM. ZO-1 in corneal epithelium; stratal distribution and synthesis induction by outer cell removal. *Exp Eye Res.* 1993;57(3):283–292.

36. Langbein L, Grund C, Kuhn C, et al. Tight junctions and compositionally related junctional structures in mammalian stratified epithelia and cell cultures derived therefrom. *Eur J Cell Biol.* 2002; 81(8):419–435.
37. Ban Y, Cooper LJ, Fullwood NJ, et al. Comparison of ultrastructure, tight junction-related protein expression and barrier function of human corneal epithelial cells cultivated on amniotic membrane with and without air-lifting. *Exp Eye Res.* 2003;76:735–743.
38. Mosmann T. Rapid colorimetric assay for cellular growth and survival: Application to proliferation and cytotoxicity assays. *Journal of Immunological Methods.* 1983;65:55–63.
39. European Centre for Ecotoxicology & Toxicology of Chemicals (ECETOC). ECETOC Technical Report No 48, Eye Irritation: Reference Chemicals Data Bank, 2nd ed. Brussels, Belgium: ECETOC; 1998.
40. Cotovio J, Grandidier MH, Amselem C, et al. The use of the SkinEthic Human Corneal Epithelial (HCE) model to predict ocular irritancy: optimized 1H/16H protocol applied to a large set of 400 industrial chemical. *AATEX Spec Issue.* 2008:343–335.
41. Jester JV, Li HF, Petroll WM, et al. Area and depth of surfactant-induced corneal injury correlates with cell death. *Invest Ophthalmol Vis Sci.* 1998;39:922–936.
42. Jester JV, Petroll WM, Bean J, et al. Area and depth of surfactant-induced corneal injury predicts extent of subsequent ocular responses. *Invest Ophthalmol Vis Sci.* 1998;39:2610–2625.
43. Maurer JK, Parker RD, Petroll WM, et al. Quantitative measurement of acute corneal injury in rabbits with surfactants of different type and irritancy. *Toxicol Appl Pharmacol.* 1999;158:61–70.
44. Jester JV, Molai A, Petroll WM, et al. Quantitative characterization of acid- and alkali-induced corneal injury in the low-volume eye test. *Toxicol Pathol.* 2000;28:668–678.
45. Jester JV, Li L, Molai A, Maurer JK. Extent of initial corneal injury as a basis for alternative eye irritation tests. *Toxicol In Vitro.* 2001;15:115–130.
46. Maurer JK, Molai A, Parker RD, et al. Pathology of ocular irritation with bleaching agents in the rabbit low-volume eye test. *Toxicol Pathol.* 2001;29:308–319.
47. Maurer JK, Molai A, Parker RD, et al. Pathology of ocular irritation with acetone, cyclohexanol, parafluoroaniline, and formaldehyde in the rabbit low-volume eye test. *Toxicol Pathol.* 2001;29:187–199.
48. Lapalus P, Garrafo R. Ocular pharmacokinetics. In: Hockwin O, Green K and Rubin LF: Gustav Fischer, eds. *Manual of Oculotoxicity Testing of Drugs*. New York: Verlag; 1992:119–136.
49. Suzuki K, Tanaka T, Enoki M, Nishida T. Coordinated reassembly of the basement membrane and junctional proteins during corneal epithelial wound healing. *Invest Ophthalmol Vis Sci.* 2000;41: 2495–2500.
50. Sugrue SP, Zieske JD. ZO1 in corneal epithelium: association to the zonula occludens and adherens junctions. *Exp Eye Res.* 1997;64: 11–20.
51. Crewe JM, Armitage WJ. Integrity of epithelium and endothelium in organ-cultured human corneas. *Invest Ophthalmol Vis Sci.* 2001;42:1757–1761.
52. Ban Y, Dota A, Cooper LJ, et al. Tight junction-related protein expression and distribution in human corneal epithelium. *Exp Eye Res.* 2003;76:663–669.
53. Yi X, Wang Y, Yu FS. Corneal epithelial tight junctions and their response to lipopolysaccharide challenge. *Invest Ophthalmol Vis Sci.* 2000;41:4093–4100.
54. Sosnovà-Netukovà M, Kuchynka P, Forester JV. The suprabasal layer of cornea epithelial cells represents the major barrier site to the passive movement of small molecules and trafficking leukocytes. *Br J Ophthalmol.* 2007;91:372–378.
55. Chuang EY, De Quan L, Bian F, Zheng X, Pflugfelder SC. Effects of contact lens multipurpose solutions on human cornea epithelial survival and barrier function. *Eye Contact Lens.* 2008;34(5):281–286.
56. Araki-Sasaki K, Ohashi Y, Sasabe T, et al. An SV40-immortalized human corneal epithelial cell line and its characterization. *Invest. Ophthalmol Vis Sci.* 1995;36:614–621.
57. Reichl R. Cell culture models of the human cornea: a comparative evaluation of their usefulness to determine ocular drug absorption in-vitro. *J Pharm Pharmacol.* 2008;60(3):299–307.
58. Becker U, Ehrhardt C, Schneider M, et al. A comparative evaluation of corneal epithelial cell cultures for assessing ocular permeability. *Altern Lab Anim.* 2008;36(1):33–44.
59. Ebato B, Friend J, Thoft RA. Comparison of limbal and peripheral human corneal epithelium in tissue culture. *Invest Ophthalmol Vis Sci.* 1988;29:1533–1537.
60. Iwata M, Fushimi N, Suzuki Y, et al. Intercellular adhesion molecule-1 expression on human corneal epithelial outgrowth from limbal explant in culture. *Br J Ophthalmol.* 2003;87:203–207.
61. Joyce NC, Navon SE, Roy S, Zieske JD. Expression of cell cycle-associated proteins in human and rabbit corneal endothelium in situ. *Invest Ophthalmol Vis Sci.* 1996;37:1566–1575.
62. Ajani G, Sato N, Mack JA, Maytin EV. Cellular responses to disruption of the permeability barrier in a three-dimensional organotypic epidermal model. *Exp Cell Res.* 2007;313:3005–3015.
63. Neppelberg E, Costea DE, Vintermyr OK, Johannessen AC. Dual effects of sodium lauryl sulphate on human oral epithelial structure. *Exp Dermatol.* 2007;16:574–549.
64. Schwab IR, Linberg JV, Gioia VM, Benson WH, Chao GM. Foreshortening of the inferior conjunctival fornix associated with chronic glaucoma medications. *Ophthalmology.* 1992;99:197–202.
65. Jaenen N, Baudouin C, Pouliquen P, et al. Ocular symptoms and signs with preserved and preservative-free glaucoma medications. *Eur J Ophthalmol.* 2007;17:341–349.
66. Baudouin C, Liang H, Hamard P, et al. The ocular surface of glaucoma patients treated over the long term expresses inflammatory markers related to both T-helper 1 and T-helper 2 pathways. *Ophthalmology.* 2008;115:109–115.